

**Cosmic Ray Proton and Helium Spectra -- Results from the JACEE Experiment**

K. Asakimori<sup>1</sup>, T.H. Burnett<sup>2</sup>, M.L. Cherry<sup>3</sup>, K. Chevli<sup>4</sup>, M.J. Christl<sup>5</sup>, S. Dake<sup>6</sup>,  
J.H. Derrickson<sup>5</sup>, W.F. Fountain<sup>5</sup>, M. Fuki<sup>7</sup>, J.C. Gregory<sup>4</sup>, T. Hayashi<sup>8</sup>, R. Holynski<sup>9</sup>,  
J. Iwai<sup>2</sup>, A. Iyono<sup>10</sup>, J. Johnson<sup>4</sup>, M. Kobayashi<sup>11</sup>, J.Lord<sup>2</sup>, O. Miyamura<sup>12</sup>,  
K.H. Moon<sup>5\*</sup>, B.S. Nilsen<sup>3</sup>, H. Oda<sup>6</sup>, T. Ogata<sup>13</sup>, E.D. Olson<sup>2</sup>, T.A. Parnell<sup>5</sup>,  
F.E. Roberts<sup>5</sup>, K. Sengupta<sup>3x</sup>, T. Shiina<sup>4</sup>, S.C. Strausz<sup>2</sup>, T. Sugitate<sup>12</sup>, Y. Takahashi<sup>4</sup>,  
T. Tominaga<sup>12</sup>, J.W. Watts<sup>5</sup>, J.P. Wefel<sup>3</sup>, B. Wilczynska<sup>9</sup>, H. Wilczynski<sup>9</sup>, R.J. Wilkes<sup>2</sup>,  
W. Wolter<sup>9</sup>, H. Yokomi<sup>14</sup>, E. Zager<sup>2</sup>

1. Kobe Women's Junior College, Kobe, Japan
2. Dept. of Physics, Univ. of Washington, Seattle, WA 98195
3. Dept. of Physics and Astronomy, Louisiana State Univ., Baton Rouge, LA 70803
4. College of Science, Univ. of Alabama, Huntsville, AL 35899
5. NASA Marshall Space Flight Center, Huntsville, AL 35812
6. Kobe Univ., Kobe, Japan
7. Kochi Univ., Kochi, Japan
8. Waseda Univ., Tokyo, Japan
9. Inst. for Nuclear Physics, Krakow, Poland
10. Okayama Univ. of Science, Okayama, Japan
11. KEK, Tsukuba, Japan
12. Hiroshima Univ., Hiroshima, Japan
13. Inst. for Cosmic Ray Research, Tokyo, Japan
14. Tezukayama Univ., Nara, Japan

**ABSTRACT**

Measurements are presented of the cosmic ray hydrogen and helium spectra at energies from 2 to 800 TeV. The experiments were performed on a series of twelve balloon flights, including several long duration Australia-to-South America and Antarctic circumpolar flights. No clear evidence is seen for a spectral break. Both the hydrogen and helium spectra are consistent with power laws over the entire energy range, with integral spectral indices  $1.80 \pm 0.04$  and  $1.68^{+0.04}_{-0.06}$  for the protons and helium respectively. The results are fully consistent with expectations based on supernova shock acceleration coupled with a "leaky box" model of propagation through the Galaxy.

**1. INTRODUCTION**

One of the striking features of high energy cosmic rays is the power law dependence of the observed flux on energy over approximately 10 orders of magnitude – from near  $10^{10}$  eV where the earth's geomagnetic field becomes transparent to the incident cosmic ray beam to  $3 \times 10^{20}$  eV, the highest energy observed by the Fly's Eye experiment (Bird et al., 1993). In the middle of this wide range of energies, however, a "knee" is observed near  $10^{15}$  -  $10^{16}$  eV where the spectrum steepens. It is not clear whether this steepening is due to

- i) a change in the acceleration mechanism at the cosmic ray source(s) possibly related to a maximum energy available from shock acceleration in galactic

- supernova remnants,
- ii) a change in the propagation mechanism, e.g., escape from the galaxy's magnetic fields,
  - iii) a change in the elemental composition of the cosmic rays,
  - iv) a change in the interaction characteristics due to new particle physics at energies  $\sqrt{s}$  above 1 TeV/nucleon,
  - v) an observational bias related to a change in the experimental techniques from direct particle-by-particle balloon and spacecraft measurements below  $\sim 10^{14}$  eV to indirect ground-based air shower measurements above  $10^{15}$  eV, or
  - vi) uncertainties in the energy determination and calibration of the air shower measurements.

In order to address these questions, to provide overlap between the direct “low energy” observations and the indirect “high energy” measurements, and to anchor the high energy air shower measurements firmly, it is necessary to push the balloon-borne direct measurements up in energy as far as possible. Long Duration Balloon (LDB) flights of large-area nuclear emulsion chambers provide the capability to perform this measurement almost to the knee region.

The high energy cosmic ray spectrum is relevant to understanding the acceleration mechanism(s) and conditions at the source(s), the propagation of the energetic cosmic rays through the galaxy, the cosmological issues of galactic vs. extragalactic origin, and the particle physics of interactions in the earth's atmosphere (and in the case of underground and underwater detectors, the earth's surface and oceans). The steepening of the all-particle spectrum above the knee, and the intensity enhancement observed below the knee (both derived indirectly from air shower data) have been the subject of numerous speculations on the acceleration and propagation mechanisms of galactic cosmic rays.

If these mechanisms depend on particle rigidity, a change in the proton energy spectrum is expected at an energy lower than that of any  $Z > 1$  component and lower than any bend in the all-particle spectrum. The first measurements in the TeV region, made by the PROTON satellites (Grigorov et al., 1971), indicated that the proton integral spectral index changed from 1.7 to 2.1 at around 2 TeV and continued constant up to at least 20 TeV. The later JACEE (Japanese-American Cooperative Emulsion Experiment) data (Burnett et al., 1983, 1990) showed no steepening up to approximately 100 TeV based on data from a series of six balloon flights. In 1991, however, JACEE reported preliminary results of the long duration Australia-to-South America JACEE 7 and 8 flights, and showed that the proton flux above 80 TeV was almost 3 standard deviations below the intensity expected from a single power law (Asakimori et al., 1991). With the fully analyzed data from JACEE 7 and 8 (cumulative exposure  $305 \text{ m}^2\text{-hrs}$ ), a “roll-over” in the proton spectrum above  $\sim 40$  TeV was indicated, but no complementary steepening was observed in the helium spectrum (Asakimori et al., 1993). The Sokol group (Ivanenko et al., 1990) reported a proton spectral index that steepened by approximately 1 standard deviation between 2.5 and 10 TeV, and a helium index that *flattened* by 1 in the same energy range. Other groups (Kawamura et al., 1989; Ivanenko et al., 1993; Zatsepin et al.,

1993) have reported no steepening in the spectra, but have agreed that the H/He ratio decreases with increasing energy.

If a bend in the proton spectrum is interpreted as due to a maximum rigidity for the acceleration process, then the helium should show a similar bend at a kinetic energy  $Z/A$  times the proton break energy; i.e., a bend in the proton spectrum near 40 TeV should appear in the helium spectrum near 20 TeV/nucleon. A steepening of the proton spectrum at some energy  $E_p$  without a corresponding steepening for helium could imply that the theoretical prediction for a maximum total energy/nucleon  $\sim ZE_p/A$  from a supernova shock is oversimplified, or it could suggest that the protons and helium come from different sources. It was clearly recognized by Asakimori et al. (1993) that the JACEE 1-8 results were statistics limited, and that additional LDB exposures would be needed to properly address the question of the high energy proton and helium spectra. We here present the results of the analysis through JACEE flight 12, with a factor of two more data than were available through JACEE 8 and with an improved treatment of systematic effects. The present results update and replace our earlier JACEE proton and helium results.

## II. EXPERIMENTAL PROCEDURE

Nuclear emulsion has the advantage that relatively light, large area, passive payloads can be flown on high altitude balloons. In order to accumulate the required high energy statistics, JACEE has now flown emulsion chambers on fifteen balloon flights (eight 1-2 day turn-around flights, two 5-6 day Australia-South America flights, and five 9-15 day Antarctic circumpolar flights, Wilkes et al., 1995). All but one of these have been successfully recovered. The total accumulated exposure is 1436 m<sup>2</sup>-hrs (Table 1). The average flight altitude ranges from 3.5 to 5.5 g/cm<sup>2</sup>. A single flight typically carries 2-6 emulsion blocks, each generally 40 x 50 cm<sup>2</sup>. Fifty-eight emulsion blocks have been flown, and fifty-two recovered. We report here on the analysis of the data from JACEE flights 1-12, covering the results from the first forty emulsion blocks (cumulative exposure 644 m<sup>2</sup>-hrs). The total number of high energy events available for analysis from all flights is  $\sim 2 \times 10^4$ . Of these,  $\sim 180$  have energy exceeding 100 TeV per particle. The present analysis is based on 656 protons above 6 TeV and 414 helium nuclei above a total energy of 8 TeV per particle.

The basic detector used in the JACEE experiments (Burnett et al., 1986; Fig. 1) is a fine-grained emulsion chamber containing approximately a hundred track-sensitive nuclear emulsion plates and a three-dimensional emulsion/X-ray film/lead plate calorimeter. (JACEE 3 was a hybrid experiment which combined the standard emulsions with a set of electronic Cerenkov detectors, proportional and ionization chambers, and a plastic shower counter in order to test the validity of the emulsion chamber approach.)

The lower part of the chamber is the calorimeter section, consisting of  $\sim 20$  layers of emulsions and X-ray films interleaved with up to 8.5 radiation lengths of 1-2.5 mm thick lead plates. The calorimeter records single charged particle tracks with a spatial

Table 1. JACEE Balloon Flights

Flight	Launch Date	Launch Site	Altitude (g/cm <sup>2</sup> )	Duration (hrs)	Units (cm x cm)	Cumulative Exposure (m <sup>2</sup> -hrs)
JACEE 0	5/79	Sanriku, Japan	8.0	29.0	1 (40 x 50)	6
JACEE 1	9/79	Palestine, TX	3.7	25.2	4 (40 x 50)	26
JACEE 2	10/80	Palestine, TX	4.0	29.6	4 (40 x 50)	50
JACEE 3	6/82	Greenville, SC	5.0	39.0	1 (50 x 50)	59
JACEE 4	9/83	Palestine, TX	5.0	59.5	4 (40 x 50)	107
JACEE 5	10/84	Palestine, TX	5.0	15.0	4 (40 x 50)	119
JACEE 6	5/86	Palestine, TX	4.0	30.0	4 (40 x 50)	143
JACEE 7	1/87	Alice Springs, Australia	5.5	150.0	3 (40 x 50)	233
JACEE 8	2/88	Alice Springs	5.0	120.0	3 (40 x 50)	305
JACEE 9	10/90	Ft. Sumner, NM	4.0	44.0	4 (40 x 50)	340
JACEE 10	12/90	McMurdo, Antarctica	3.5	204.0	2 (30 x 40)	389
JACEE 11	12/93	McMurdo	4.5	217.0	6 (40 x 50)	*
JACEE 12	1/94	McMurdo	5.0	212.0	6 (40 x 50)	644
JACEE 13	12/94	McMurdo	5.0	310.0	6 (40 x 50)	1016
JACEE 14	12/95	McMurdo	5.0	350.0	6 (40 x 50)	1436

\* JACEE 11 was lost in the ocean due to a malfunction at shutdown after a nine day flight.

resolution in the emulsion of better than 1  $\mu\text{m}$ , and individual photon cascades with a resolution of a few microns. High energy showers produce visible dark spots in the X-ray film, which are used to locate and trace the energetic cascades. On average, more than 400 events are detected per block with optical density in the electromagnetic cascade

( $D_{\text{max}}$  for a slit size of 200  $\mu\text{m}$  x 200  $\mu\text{m}$ ) greater than 0.2, corresponding to a total energy in the electromagnetic shower  $E \approx 1.5$  TeV for protons. In the original JACEE analyses (Burnett et al., 1986, 1990; Asakimori et al., 1991, 1993), electron counts in the emulsion layers along the cascade were compared to a simulated shower development curve to determine the total electromagnetic energy  $E$  deposited in the calorimeter. The electron counting in the emulsion is a slow, manual, manpower-intensive operation. In order to speed up the analysis for the large new data sample obtained from our long duration Antarctic flights, we have derived  $E$  directly from the darkness  $D$  measured in the X-ray films. X-ray film optical density is defined in terms of the fraction of incident light intensity transmitted through a sample

$$D = -\log I/I_0 \quad (1)$$

Measured film density  $D$  is then related to the density of electron tracks  $n$  in an adjacent emulsion plate by the empirical relation (Ohta et al., 1979)

$$D = D_o \left(1 - \frac{1}{1 + n}\right) \quad (2)$$

where the constant  $D_o$  is determined from measurements with a calibration wedge, and is determined by a calibration of  $D$  with direct counting of the shower electron density. The net density or "darkness" due to a shower electron density  $n_s$ , superimposed on a background  $n_b$ , is

$$D_{\text{net}} = D_{\text{total}} - D_{\text{bkg}} = D_o \frac{1}{1 + n_b} - \frac{1}{1 + (n_s + n_b)} \quad (3)$$

where the background density  $n_b$  is determined from Eq. 2 with  $n = n_b$  and  $D = D_{\text{bkg}}$  measured away from the shower spot. The shower electron density is determined at various points along the track of the shower either directly by counting in the emulsion or indirectly from the X-ray film darkness. Corrections are made for non-vertical angles, shadowing of the bottom layer of the film by the top layer, and the finite film thickness, and  $n_s$  is then fitted to the electromagnetic shower development curves in order to determine  $E$  (Burnett et al., 1986; Olson, 1995).

A correction must be made for both background and saturation in the X-ray film densitometry. This is especially important for the Antarctic LDB flights, where fogging due to the low geomagnetic cutoff rigidity, the long flight duration, and in a few cases somewhat old X-ray films tended to increase the background levels and decrease dynamic range. We use neutral density filters to increase the dynamic range. In the absence of filtering,  $D_o = 4.2$  due to photomultiplier saturation; with proper filters,  $D_o = 6.5$  due to film saturation. For JACEE 12, the observed background level was  $D_{\text{bkg}} \sim 1.6$  (higher by 0.5 - 1 unit than in previous flights). Therefore, in order to reduce the effect of saturation, all high-D JACEE 12 showers were measured with a  $D = 1.4$  filter.

It should be noted that the definition of  $n_s$  in terms of the net darkness in Eq. 3 is somewhat different from the standard convention, where  $D_{\text{net}}$  is set equal to  $D$  in Eq. 2 (Ohta et al., 1979; Okamoto et al., 1981; Kasahara et al., 1985; Kawamura et al., 1989). The two definitions give similar numerical results for  $n_b \ll 1$ . For high energy measurements which employ data from long duration balloon or mountain-top exposures, however, the use of the proper characteristic curve (Eq. 3) for  $D_{\text{net}}(n_s)$  is important. As an example, for a long duration JACEE 12 data sample with  $D_{\text{bkg}} = 1.6$  and  $D_{\text{net}} = 1.0$ , the darkness calculation without the background correction (e.g., Eq. 2) underestimates  $E$  by 4%. At  $D_{\text{net}} = 1.2$ , however, there is a 30% underestimate for vertically incident particles and 21% underestimate for particles with zenith angle  $\theta = 79^\circ$  ( $\tan \theta = 5.0$ ). The characteristic curve without background correction has been used by the JACEE

group for the analysis of its shorter flights until 1993. In the present analysis, the data have been reanalyzed using the correct expression (Eq. 3) for all values of darkness.

In practice, the value determined from the densitometry is the maximum darkness  $D_{\max}$ , i.e., the film darkness at shower maximum. However, the parameter  $\mu$  used in converting  $D_{\max}$  to electron counts (Eqs. 2 and 3) depends on the primary particle's angle of incidence. At darkness values near threshold, the cutoff therefore is dependent on angle and an energy-dependent efficiency correction must be applied, resulting in a background density-dependent effective threshold  $E_{\text{thresh}} \sim 700 \text{ GeV}$  ( $D_{\max} \sim 0.1$ ). The correction for incident direction becomes independent of energy above  $E \sim 4 \text{ TeV}$ . Since the tracing of each event through the emulsion layers is time-consuming, only high energy events are selected for analysis. The selection criteria require a minimum  $D_{\max}$  ranging from 0.2 for JACEE 1-6 to 0.5 for JACEE 12. Zenith angle  $\theta$ , azimuth angle  $\phi$ , and optical density  $D_{\max}$  are recorded for all selected events. A zenith angle cut is applied for each flight; typically  $\tan \theta = 5.0$  ( $\theta = 79^\circ$ ) for high energy events ( $D_{\max} > 0.5$ ) and  $\tan \theta = 3.0$  ( $\theta = 72^\circ$ ) for events with  $D_{\max} < 0.5$ . With these selection criteria, the effective solid angle acceptance of the chamber remains very high ( $\sim 3 - 3.5 \text{ sr}$ ) compared to that for a typical electronic calorimeter experiment ( $\sim 0.1 \text{ sr}$ ).

A comparison of  $E$  values determined from direct electron counting to those derived from the X-ray film densitometry (Olson, 1995; Cherry et al., 1995) gives a dispersion in the individual event  $E$  values of approximately 30% between the two methods. Shower-to-shower fluctuations (including the event-to-event variations in interaction height and the variations due to the width of the inelasticity distribution in nucleon-nucleus interactions) have been studied using Monte Carlo simulations (Burnett et al., 1986; Asakimori and Roberts, 1994). The standard deviations of the relative widths derived from the simulations are 18% and 23% for protons and helium respectively, resulting in a net uncertainty  $(\sigma_E)/E \sim 35\text{-}38\%$ .

Since the cosmic ray spectrum is approximately a power law decreasing rapidly with increasing energy, this uncertainty in the measured energy  $E$  means that low-energy particles will be preferentially misidentified as higher energy particles. If the "real"

$E$  spectrum is denoted  $dN/dE$ , then the observed spectrum will be the convolution of  $dN/dE$  with a resolution function (assumed to be Gaussian)

$$\frac{dN}{dE} = \int_0^\infty \frac{dN_0}{dE_0} \frac{e^{-\frac{1}{2} \left( \frac{E - E_0}{\sigma} \right)^2}}{\sqrt{2\pi} \sigma} dE_0 \quad (4)$$

where the proton (helium) resolution is  $\sigma/E = 0.35$  (0.38). In the case of a power law input spectrum with integral spectral index  $\alpha$  between 2 and 3, the integration (4) is carried out numerically and results in a correction to the normalization of approximately 4 - 11%.

The measured energy  $E$  is related to the primary energy  $E$  by the partial inelasticity  $k$ . Since the inelasticity distribution  $f(k)$  has a width  $\sim 50\%$ , it is not possible to determine accurately the primary energy  $E$  of an individual event. There is, however, a well-defined relation between the  $E$  spectrum and the primary spectrum (Burnett et al., 1986; Kawamura et al., 1989). As long as the primary spectrum does not change slope, and there is no change in the interaction characteristics over the energy range being considered, the primary spectrum and the  $E$  spectrum will be parallel. The primary spectrum can be determined from the  $E$  spectrum by a simple scale shift: If the primary spectrum is of the form

$$dN/dE = I_0 E^{-(\alpha+1)}, \quad (5)$$

then the measured spectrum will be

$$\begin{aligned} \frac{dN}{dE} &= \int_0^1 f(k) dk \int_0^1 (E - kE) I_0 E^{-(\alpha+1)} dE \\ &= I_0 E^{-(\alpha+1)} \int_0^1 k f(k) dk. \end{aligned} \quad (6)$$

The measured spectrum therefore has the same slope as the primary spectrum, but with a normalization that differs by a factor  $C$ , where

$$C(k, \alpha) = \int_0^1 k f(k) dk \quad (7)$$

$C(k, \alpha)$  represents the shift in the energy scale required to go from the primary spectrum to the measured  $E = C(k, \alpha) E$  spectrum. In the case where the spectral index changes, the  $dN/dE$  and  $dN/dE$  spectra are parallel above and below the break energy, and the energy of the break shifts by  $\sim 10\text{-}20\%$ . For the measured JACEE spectra presented in Sec. III, the  $C(k, \alpha)$  values for events interacting in the JACEE target section are 0.265 and 0.168 for protons and helium, respectively. For events interacting in the calorimeter, the  $C(k, \alpha)$  values are  $\sim 10\%$  higher.

The primary particle charge is measured by grain or gap counting using a combination of low sensitivity (Fuji 6B) and high sensitivity (Fuji 7B) emulsions in the upper portion of the chamber (Burnett et al., 1986, 1990). The measurement accuracy is  $Z = 0.2e$  for both protons and helium. The discrimination of protons from helium is

made with close to 100% efficiency. We note that some other emulsion chamber experiments do not have this capability. In JACEE, the use of background nuclei as fiducials makes possible a precision triangulation of the event axis. The resulting error in locating the primary track in the emulsion plates is  $\sim 10 \mu\text{m}$ , so that there are practically no spurious background tracks with the same  $(\theta, \phi)$  values within this small area, and the identification of protons and helium is essentially unique at all angles.

### III. RESULTS AND DISCUSSION

Figure 2 shows the measured JACEE 1-12 integral spectra  $N(>E)$  for hydrogen and helium, including an atmospheric correction and corrections for the interaction height, target volume, and geometry for each particular event. Each point on the plot corresponds to one more event than the point to the right. The wavy shape of the low- statistics high-energy points (e.g., the dip in the proton spectrum between 60 and 100 TeV, and in the helium spectrum near 20 - 30 TeV) is characteristic of the point-to-point correlations in an integral plot. The straight lines shown in Fig. 2 are maximum likelihood fits with power law indices

$$\alpha_{\text{H}} = 1.80 \pm 0.04 \qquad \alpha_{\text{He}} = 1.68^{+0.04}_{-0.06}. \qquad (8)$$

The JACEE 1-12 data are consistent with a single power law over the entire energy range. With the increased statistics, although we cannot rule out the two-component spectrum of Asakimori et al. (1993), we nevertheless see no evidence for a break in the spectrum. The hydrogen spectrum appears to be steeper than that of the helium, with a difference between the spectral indices of  $0.12 \pm 0.06$ .

The differential spectra  $dN/dE$  shown in Fig. 3 demonstrate that the normalization agrees with the lower energy data. The solid lines shown in Fig. 3 are the fits to the JACEE spectra:

$$\begin{aligned} dN/dE_{\text{H}} &= (1.11^{+0.08}_{-0.06}) \times 10^{-1} E^{-2.80 \pm 0.04} \quad (\text{m}^2\text{-sr-s-TeV})^{-1} \\ dN/dE_{\text{He}} &= (7.86 \pm 0.24) \times 10^{-3} E^{-2.68^{+0.04}_{-0.06}} \quad (\text{m}^2\text{-sr-s-TeV/n})^{-1} \end{aligned} \qquad (9)$$

If we assume a standard ‘‘leaky box’’ model for the cosmic ray propagation (Ormes and Freier, 1978; Cesarsky, 1980) then the measured secondary-to-primary cosmic ray ratios lead to an energy-dependent cosmic ray pathlength through the galaxy (Garcia-Munoz et al., 1984, 1987; Guzik and Wefel, 1984), for example

$$R = \frac{R}{R_0} + \dots, \qquad (10)$$

where  $R = pc/Ze$  is the particle rigidity,  $\rho_0 = 6 \text{ g/cm}^2$ ,  $R_0 = 10 \text{ GV}$ , and  $\beta = 0.6$ . The constant term  $\rho_1$  is required by the absence of anisotropy at high energies (Swordy, 1995). At energies in the TeV range, where the pathlength  $l$  is small compared to the interaction mean free path, the leaky box model predicts hydrogen and helium spectra of the form  $dN/dE \sim E^{-\alpha}$  where  $E^{-\alpha}$  is the source spectrum. As long as  $l$  is small compared to  $\rho_0 (R/R_0)^{-\beta}$ , the observed spectra should be of the form  $dN/dE \sim E^{-\alpha-6}$ . The measurements therefore suggest source spectra of the form

$$\left. \frac{dN}{dE} \right|_{\text{source,H}} \sim E^{-2.2} \quad \left. \frac{dN}{dE} \right|_{\text{source,He}} \sim E^{-2.1} \quad (11)$$

A helium spectrum slightly flatter than that of the hydrogen is consistent both with the non-linear shock acceleration calculations of Ellison (1993) and the multiple source models of Biermann (1993) and others, which suggest supernova remnant shock acceleration from a supernova exploding into the interstellar medium to explain the hydrogen spectrum, and a supernova exploding into the stellar wind of the pre-supernova star (e.g. a Wolf-Rayet star) to explain the high energy helium.

At the energy where  $l \sim \rho_0 (R/R_0)^{-\beta}$ , the presence of the constant term  $\rho_1$  in Eq. (11) implies that both the hydrogen and the helium spectra should flatten to  $dN/dE \sim E^{-\alpha}$ . As long as the shock acceleration region is sufficiently large that the accelerator has not yet reached its maximum energy, the spectra will flatten toward the source spectra. The absence of any observed flattening by 200 TeV implies that  $\rho_1 < 0.016 \text{ g/cm}^2$ .

The maximum proton energy expected from acceleration at a parallel shock, assuming the standard value of  $3\mu\text{G}$  for the interstellar magnetic field, is  $E_p \sim 100 \text{ TeV}$  (Lagage and Cesarsky, 1983). This value can be extended upward by employing quasi-perpendicular shocks (Jokipii, 1987) or higher magnetic fields, as might be encountered by a supernova remnant expanding into the wind of a massive progenitor star (Völk and Biermann, 1988). Likewise, reacceleration by multiple supernova remnants (Axford, 1991) or a galactic termination shock (Jokipii and Morfill, 1991) might significantly increase  $E_p$ . The absence of a spectral break in the present results near 100 TeV can therefore be readily accommodated by extensions to the original Lagage and Cesarsky (1983) model.

#### IV. CONCLUSIONS

The JACEE results represent the highest energy direct particle-by-particle measurements available on the spectrum of cosmic ray hydrogen and helium up to 800 TeV. With 644  $\text{m}^2\text{-hrs}$  of accumulated exposure (including the results from two  $>200 \text{ hr}$  Antarctic flights), we have measured 656 proton events above 6 TeV and 414 heliums above 2 TeV/nucleon. The resulting spectra are consistent with power laws with no spectral breaks. The hydrogen spectral index is steeper than that of the helium by 0.12, corresponding to 2 standard deviations. With the improved statistics from the Antarctic

flights, the results appear to be consistent with the predictions based on models of supernova shock acceleration and leaky box propagation.

## V. ACKNOWLEDGMENTS

This work has been supported in the US by NASA (Space Physics, EPSCoR), the National Science Foundation (Particle Physics, Polar Programs, EPSCoR), Department of Energy (High Energy Physics), the State of Alabama EPSCoR program, and the Louisiana Board of Regents; in Japan by the Institute for Cosmic Ray Research, University of Tokyo, Japan Soc. for Promotion of Science, Yamada Science Foundation, and the Kashima Foundation; and in Poland by the Polish State Committee for Scientific Research and the Maria Sklodowska-Curie Fund (grants 2P03B18109 and PAA/NSF-96-256). We appreciate the extensive microscope work by A. Aranas, B.-L. Dong, and S. Toyoda.

\* Deceased

× Present address: Horizon Computer Corp., 5 Lincoln Highway, Edison, N.J. 08820

## REFERENCES

- Anand, K.C. *et al.* 1968, *Canad. J. Phys.* **46**, 5652.  
Asakimori, K. *et al.* 1991, *Proc. 22nd Intl. Cosmic Ray Conf.* (Dublin) **2**, 97.  
Asakimori, K. *et al.* 1993, *Proc. 23rd Intl. Cosmic Ray Conf.* (Calgary) **2**, 21 and **2**, 25.  
Axford, W.I. 1991, in *Astrophysical Aspects of the Most Energetic Cosmic Rays*, ed. by M. Nagano and F. Takahara (World Scientific: Singapore), p. 406.  
Badhwar, G.D. *et al.* 1977, *Proc. 15th Intl. Cosmic Ray Conf.* (Plovdiv) **11**, 155  
Biermann, P.L. 1993, *Astron. Astrophys.* **271**, 649; Biermann, P.L. and Cassinelli, J.P. 1993, *Astron. Astrophys.* **277**, 691; Biermann, P.L. and Strom, R.G. 1993, *Astron. Astrophys.* **275**, 659.  
Bird, D.J. *et al.* 1993, *Phys. Rev. Lett.* **71**, 3401.  
Burnett, T.H. *et al.* 1983, *Phys. Rev. Lett.* **51**, 1010.  
Burnett, T.H. *et al.* 1986, *Nucl. Instrum. Meth. in Physics Res.* **A251**, 583.  
Burnett, T.H. *et al.* 1990, *Ap. J.* **349**, 25.  
Cesarsky, C.J. 1980, *Ann. Rev. Astron. Astrophys.* **18**, 289.  
Cherry, M.L. *et al.* 1995, *Proc. 24th Intl. Cosmic Ray Conf.* (Rome) **2**, 728.  
Dwyer, J. *et al.* 1993, *Proc. 23rd Intl. Cosmic Ray Conf.* (Calgary) **1**, 587.  
Ellison, D.C. 1993, *Proc. 23rd Intl. Cosmic Ray Conf.* (Calgary) **2**, 219.  
Freier, P.S. and Waddington, C.J., 1968, *JGR* **264**, 4261.  
Garcia-Munoz, M. *et al.* 1984, *Ap. J. Lett.* **280**, L13.  
Garcia-Munoz, M. *et al.* 1987, *Ap. J. Suppl.* **64**, 269.  
Grigorov, N.L. *et al.* 1971, *Proc. 12th Intl. Cosmic Ray Conf.* (Hobart) **5**, 1746.  
Grigorov, N.L. *et al.* 1990, *Proc. 21st Intl. Cosmic Ray Conf.* (Adelaide) **3**, 73; and Grigorov, N.L. 1990, *Sov. J. Nucl. Phys.* **51**, 99.  
Guzik, T.G. and Wefel, J.P. 1984, *Adv. Space Res.* **4**, 215.

- Ichimura, M. *et al.* 1993, *Phys. Rev.* **D48**, 1949.
- Ivanenko, I.P. *et al.* 1990, *Proc. 21st Intl. Cosmic Ray Conf.* (Adelaide) **3**, 77.
- Ivanenko, I.P. *et al.* 1993, *Proc. 23rd Intl. Cosmic Ray Conf.* (Calgary) **2**, 17.
- Jokipii, J.R. 1987, *Ap. J.* **313**, 842.
- Jokipii, J. R. and Morfill, G. 1991, in *Astrophysical Aspects of the Most Energetic Cosmic Rays*, ed. by M. Nagano and F. Takahara (World Scientific: Singapore), p. 261.
- Kasahara, K. *et al.* 1985, *Phys. Rev.* **D31**, 2737.
- Kawamura, Y. *et al.* 1989, *Phys. Rev.* **D40**, 729.
- Lagage, P.O. and Cesarsky, C.J. 1983, *Astron. Astrophys.* **118**, 223 and **125**, 249.
- Ohta, I. *et al.* 1979, *Nucl. Instrum. Meth.* 1979, **161**, 35.
- Okamoto, T. *et al.* 1981, *Proc. 17th Intl. Cosmic Ray Conf.* (Paris) **5**, p. 214, p. 218, p. 222.
- Olson, E.D. 1995, Ph.D. thesis, Univ. of Washington.
- Ormes, J.F. and Freier, P.S. 1978, *Ap. J.* **222**, 471.
- Ramaty, R. *et al.* 1973, *Science* **180**, 731.
- Ryan, M.J. *et al.* 1972, *Phys. Rev. Lett.* **28**, 985.
- Seo, E.S. *et al.* 1991, *Ap. J.* **378**, 763.
- Smith, L.H. *et al.* 1973, *Ap. J.* **180**, 978.
- Swordy, S.P. 1995, *Proc. 24th Intl. Cosmic Ray Conf.* (Rome) **2**, 697.
- Swordy, S.P. *et al.* 1995, *Proc. 24th Intl. Cosmic Ray Conf.* (Rome) **2**, 652.
- Takahashi, Y. 1979, *AIP Conf. Proc.* **49**, *Cosmic Rays and Particle Physics* (New York: AIP), p. 166.
- Takahashi, Y. *et al.* 1996, in *Proc. 2nd Recontres du Vietnam (The Sun and Beyond)*, ed. by Tran Thanh Van (World Scientific: Singapore).
- Verma, R.P. *et al.* 1972, *Nature* **240**, 135.
- Völk, H.J. and Biermann, P.L. 1988, *Ap. J. Lett.* **333**, 265.
- Wilkes, R.J. *et al.* 1995, *Proc. 24th Intl. Cosmic Ray Conf.* (Rome) **3**, 615.
- Zatsepin, V.I. *et al.* 1993, *Proc. 23rd Intl. Cosmic Ray Conf.* (Calgary) **2**, 13.
- Zatsepin, V.I. *et al.* 1993, *Proc. 23rd Intl. Cosmic Ray Conf.* (Calgary) **5**, 439.

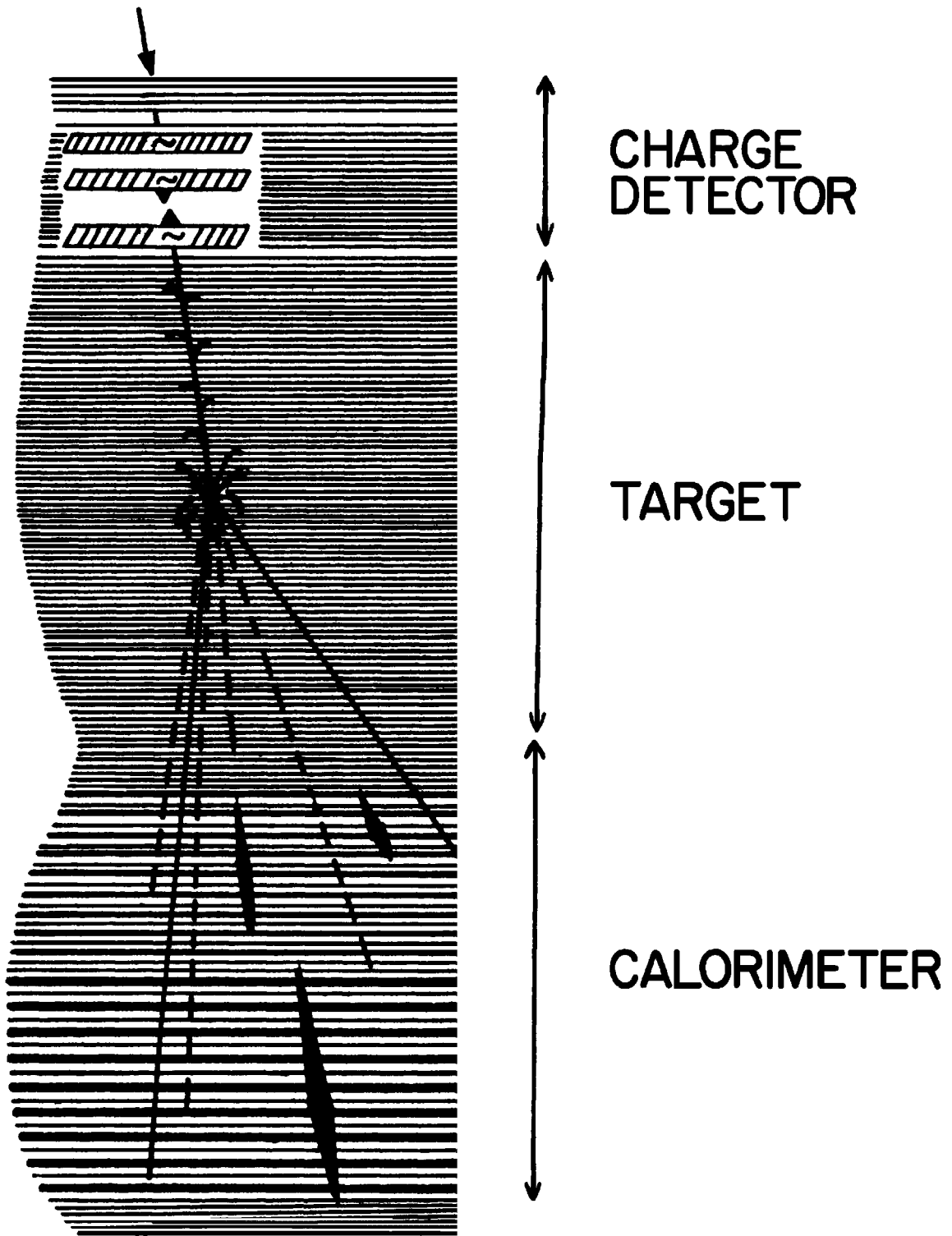


Fig. 1. Schematic diagram of the JACEE experimental configuration.

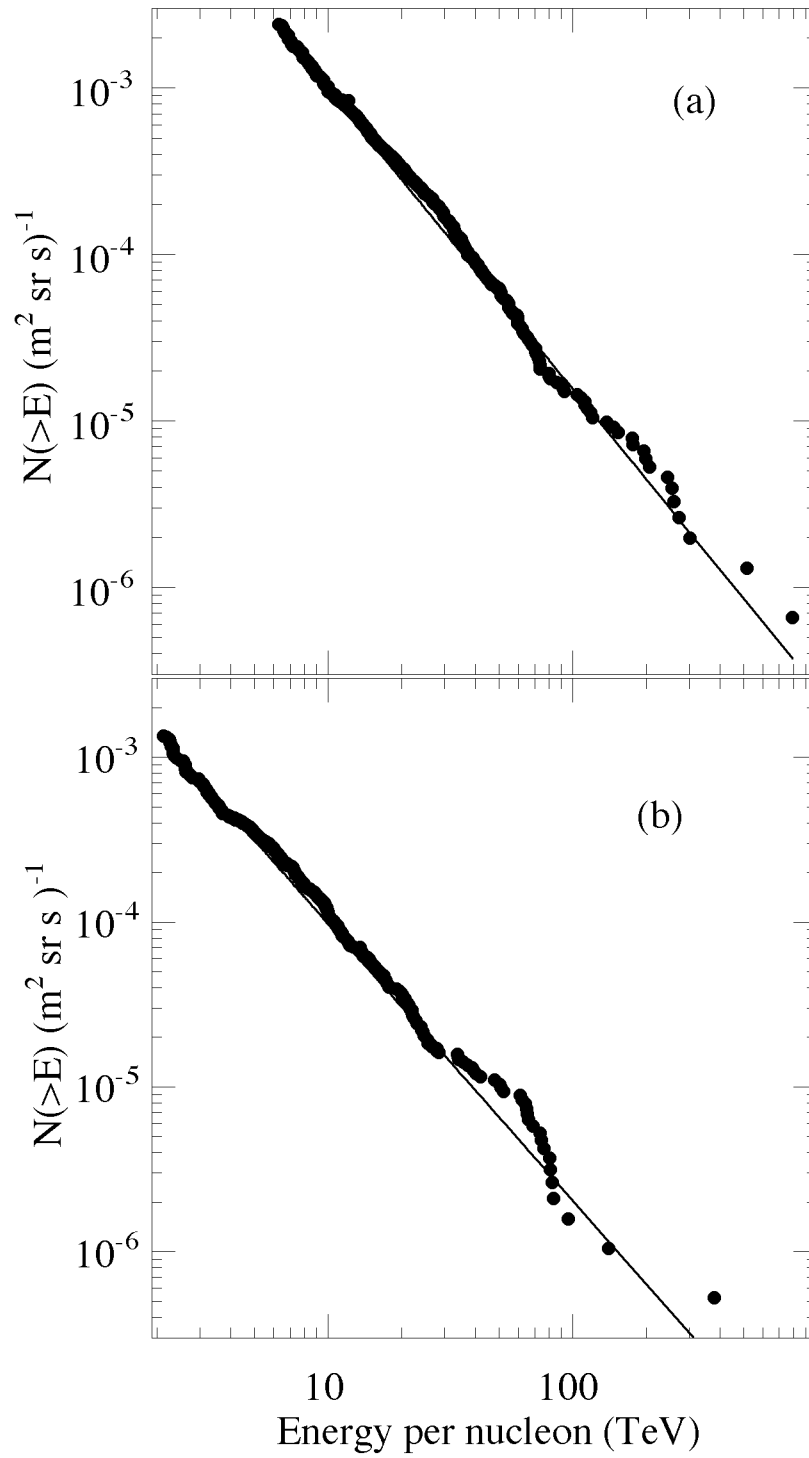


Fig. 2. Measured JACEE 1-12 integral spectrum  $N(>E)$  for hydrogen (a) and helium (b).

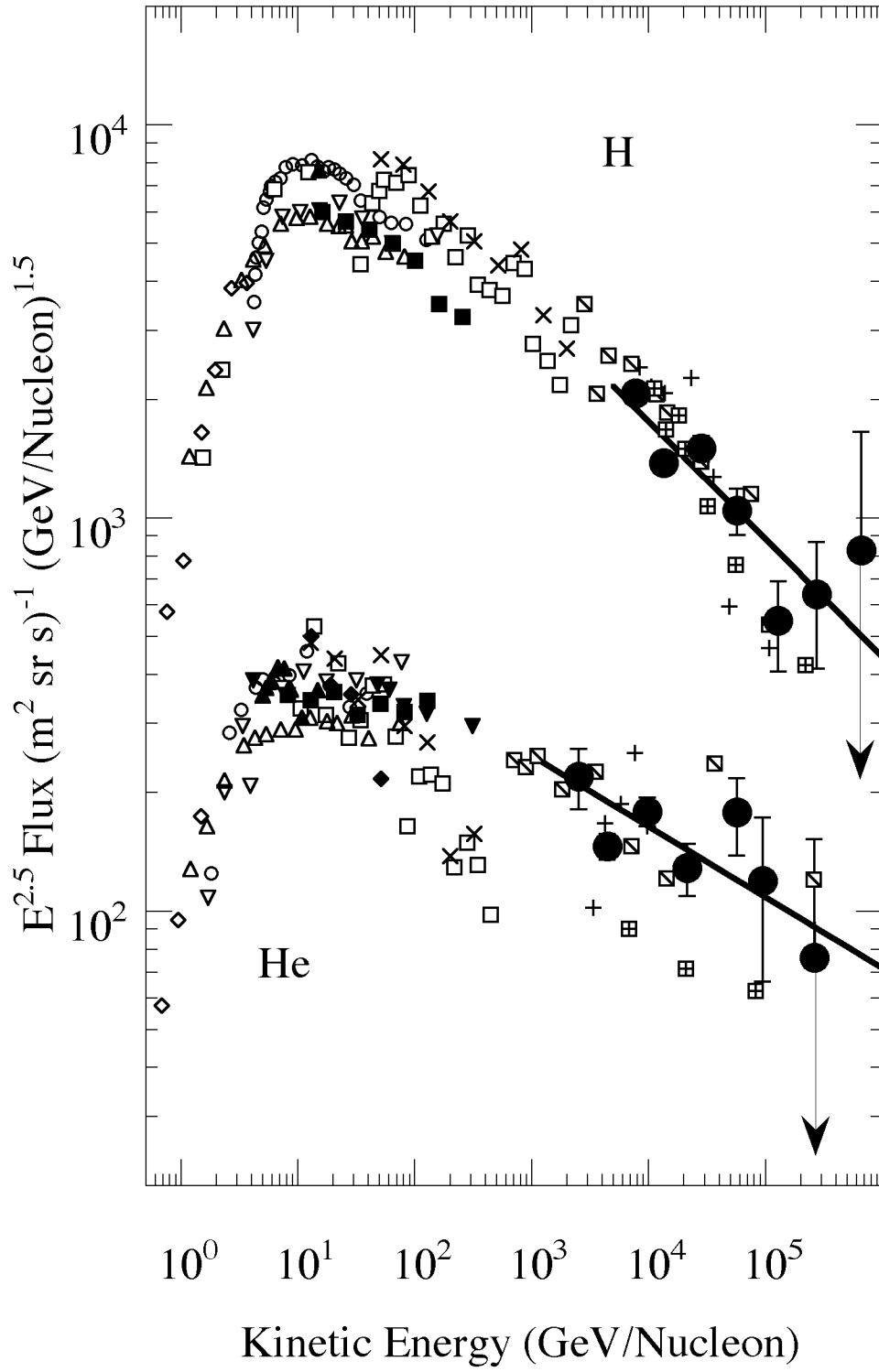


Fig. 3. Differential spectra  $dN/dE$  showing present results (l ) together with earlier results from Freier and Waddington (1968, ), Anand et al. (1968, s ), Ryan et al. (1972, ×), Verma et al. (1972, ), Ramaty et al. (1973, □), Smith et al. (1973, ), Badhwar et al. (1977, ), Seo et al. (1991, ), Dwyer et al. (1993, †), Ichimura et al. (1993, +), Ivanenko et al. (1993, ▣), Zatsepin et al. (1993, ‡), and Swordy et al. (1995, ■).